Adsorption 9: 125–132, 2003

Equilibrium and Kinetic Modelling of Adsorption of Phosphorus on Calcined Alunite

MAHMUT ÖZACAR
Department of Chemistry, Science & Arts Faculty, Sakarya University, 54100 Sakarya, Turkey
mozacar@hotmail.com

Received May 26, 2002; Revised November 14, 2002; Accepted February 19, 2003

Abstract. The adsorption of phosphorus onto calcined alunite has been studied. Its equilibrium isotherm has been measured. The isotherm was determined by shaking 1.0 g calcined alunite, particle size range 90–150 μm, with 100 mL phosphorus solution of initial concentrations from 0.5 to 2.5 mmol/L. The water bath shaking a constant rate of 200-rpm was used and the temperature maintained at 298 $\pm$ 2 K. A contact time of 120 min was required to achieve equilibrium. The experimental isotherm data were analyzed using the Langmuir, Freundlich, Temkin and Dubinin-Radushkevich equations. The monolayer adsorption capacity is 1.355 mmol P per g calcined alunite. Three simplified kinetic models including a pseudo first-order equation, pseudo second-order equation and intraparticle diffusion equation were selected to follow the adsorption process. Kinetic parameters, rate constants, equilibrium sorption capacities and related correlation coefficients, for each kinetic model were calculated and discussed. It was shown that the adsorption of phosphorus could be described by the pseudo second-order equation.

Keywords: alunite, adsorption isotherms and kinetics, phosphorus, pseudo second-order, intraparticle diffusion

1. Introduction

Phosphorus is used in many consumer products and industrial processes that involve particles of a colloidal nature. Examples of such applications are as diverse as fertilizers, detergents, pigment formulation, water treatment and mineral processing (Huynh and Jenkins, 2001; Gao and Mucci, 2001). Phosphorus discharged into the surface waters stimulates the growth of aquatic micro- and macro-organisms in nuisance quantities, which in excess can cause eutrophication in stagnant water bodies (Uğurlu and Salman, 1998). Therefore, removal of phosphorus from the wastewaters can be an effective method for the control of eutrophication in lakes and similar stagnant water bodies (Bhargava and Sheldarkar, 1993a).

There has been increasing attention towards alternative methods for phosphorus removal in wastewater treatment during the last 20 years. For several reasons, the use of inorganic adsorbents seems to be a promising alternative. Because phosphate ions are known to adsorb strongly to most metal oxides, which can strongly influence the surface chemistry of metal oxides and the availability of phosphate in natural systems. Phosphorus removal through adsorbents, such as activated alumina, fly ash, blast furnace slag, zeolite, different soils including metal oxides, goethite, pumice, titanium dioxide have been investigated (Gao and Mucci, 2001; Gong, 2001; Grubb et al., 2000; Agyei et al., 2000; Johansson and Gustafsson, 2000; Connor and McQuillan, 1999; Uğurlu and Salman, 1998; Sakadevan and Bavor, 1998; Onar et al., 1996; Brattebø and Ødegaard, 1986).

Alunite is an alternative and favorable adsorbent for phosphate due to its high capacity and selectivity. Because alunite is enriched with the oxides of aluminum and silica, alunite emerges as candidate material to treat phosphate-laden effluents since aluminum is known to strongly adsorb or precipitate phosphates in many industrial and environmental applications (Grubb et al.,

2000). However, only a limited number of studies on the use of alunite as an adsorbent have been found in the literature.

The aim of this study is to evaluate the phosphate removal potential and related kinetics of alunite due to the fact that it is a very abundant and inexpensive material in Turkey and in the world. The adsorption ability of phosphorus using alunite was investigated. The Langmuir, Freundlich, Temkin and Dubinin-Radushkevich equations were used to fit the equilibrium isotherm. Finally, the rates and mechanism of the adsorption process were investigated. Three simplified kinetic models including pseudo first- and second-order equations, and the intraparticle diffusion model were used to describe the adsorption process. These fundamental data will be useful for further applications in the treatment of practical waste or process effluents.

2. Materials and Methods

Alunite, $KAl_3(SO_4)_2(OH)_6$, is a mineral not soluble in water in its original form. It was formed by hydrothermal alteration of tuff. Therefore it contains approximately 50% SiO_2 (Şengil, 1995). Alunite used in this study was obtained from Kütahya-Şaphane, Turkey. The composition of alunite used in these studies is given in Table 1 (Özacar and Şengil, 2002). The alunite samples were treated before using in the experiments as follows (Özacar and Şengil, 2002): Alunite was prepared by grinding it in a laboratory type ball-mill. The alunite samples were calcined in muffle furnace at 1073 K for 30 min. This calcination temperature and time were found to be the optimum for phosphorus adsorption (not shown). Then it was sieved to give different particle size fractions using ASTM standard sieves, and 90–150 μm particle size was used in the experiments. The BET specific surface area was measured to be 133.3 m^2/g from N_2 adsorption isotherms with a sorptiometer (Porous Materials Inc., Model BET-202A).

Standard phosphorus solutions were prepared by dissolving the anhydrous K_2HPO_4 (Merck) in appropriate amounts in distilled water. In the determination of equilibrium adsorption isotherm, 1 g calcined alunite and 100 mL of the chosen desired concentration of K_2HPO_4 solutions were transferred in 250 mL flask, and shaken on a horizontal bench shaker (Nüve SL 250) for 120 min (the time required for equilibrium to be reached between phosphorus adsorbed and phosphorus in solution) using a bath to control the temperature at 298 ± 2 K. The experiments were performed at 200-rpm and at the initial pH 5. This pH was found to be the optimum for phosphorus adsorption onto calcined alunite in the previous experiments (not shown). The pH of the solutions was adjusted with HCl or NaOH solution by using a pH meter. At the end of the adsorption period, the samples were taken and filtered through a 0.45 μm Milipore filter paper and then the concentration of the residual phosphorus, C_e, was determined with respect to Standard Methods (APHA, 1985) with the aid of a spectrophotometer (Shimadzu UV-150-02). The measurements were made at the wavelength $\lambda = 690$ nm, which corresponds to maximum absorbance. The amount of adsorption at equilibrium, q_e (mmol/g), was computed as follows:

$$q_e = \frac{(C_0 - C_e)V}{W} \tag{1}$$

where C_0 and C_e are the initial and equilibrium solution concentrations (mmol/L), respectively, V the volume of the solution (L) and W the weight of calcined alunite used (g). Each experiment was performed twice at least under identical conditions. Reproducibility of the measurements was mostly within 3%.

In the experiments of batch kinetic adsorption, 100 mL of the chosen desired concentration of K_2HPO_4 solutions were placed in 250 mL flask together with 1 g calcined alunite and shaken by a shaker in a water bath to control temperature. At predecided intervals of time, samples were taken, and their concentrations were determined.

Table 1. The chemical composition of original alunite ore in wt.% (Özacar and Şengil, 2002).

Al_2O_3	SiO_2	SO_3	Fe_2O_3	TiO_2	CaO	MgO	K_2O	Na_2O	H_2O
20.85	48.19	17.91	0.07	0.17	0.17	0.10	4.59	0.06	7.89

3. Results and Discussion

3.1. Equilibrium Studies

Figure 1 shows the equilibrium adsorption of phosphorus (q_e versus C_e) using calcined alunite. The isotherm rises sharply in the initial stages for low C_e and q_e values. This indicates that there are plenty of readily accessible sites. Eventually a plateau is reached, indicating that the adsorbent is saturated at this level. The

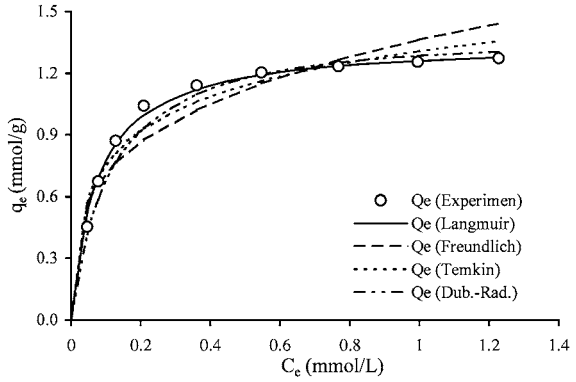

Figure 1. Equilibrium isotherms of phosphate on calcined alunite. Conditions: 90–150 μm particle size, 1073 K and 30 min calcination, 1 g/100 mL dose, 298 K temperature and pH5.

decrease in the curvature of the isotherm, tending to a monolayer, considerably increasing the C_e values for a small increase in q_e, is possibly due to the less active sites being available at the end of the adsorption process and/or the difficulty of the edge molecules in penetrating the adsorbent, phosphate molecules partially covering the surface sites.

In order to optimize the design of a sortion system to remove phosphorus from effluents, it is important to establish the most appropriate correlation for the equilibrium curve. Four isotherm equations have been tested in the present study, namely, Langmuir, Freundlich, Temkin and Dubinin-Radushkevich.

3.1.1. The Langmuir Isotherm. The widely used Langmuir isotherm (Bajpai et al., 2000; Agyei et al., 2000; Ho and McKay, 1999a; Connor and McQuillan, 1999; Sakadevan and Bavor, 1998; Onar et al., 1996) has found successful application in many real sorption processes and is expressed as:

$$q_e = \frac{K_L C_e}{1 + a_L C_e} \tag{2}$$

A linear form of this expression is:

$$\frac{C_e}{q_e} = \frac{1}{K_L} + \frac{a_L}{K_L} C_e \tag{3}$$

where q_e (mmol/g) and C_e (mmol/L) are the amount of adsorbed phosphorus per unit weight of adsorbent and unadsorbed phosphorus concentration in solution at equilibrium, respectively. The constant K_L is the Langmuir equilibrium constant and the K_L/a_L gives the theoretical monolayer saturation capacity, Q_0. Therefore a plot of C_e/q_e versus C_e gives a straight line of slope a_L/K_L and intercept $1/K_L$.

The values of the Langmuir constants a_L, K_L and Q_0 with the correlation coefficent are listed in Table 2 for the phosphorus-calcined alunite system and the Langmuir isotherm is plotted in Fig. 1 together with the experimental data points. The monolayer saturation capacity, Q_0, is 1.355 mmol/g. The value of the correlation coefficient is higher than the other three isotherms values. In all cases, the Langmuir equation represents the best fit of experimental data than the other isotherm equation (Fig. 1).

3.1.2. The Freundlich Isotherm. The well-known Freundlich isotherm (Agyei et al., 2000; Baup et al., 2000; Sakadevan and Bavor, 1998; Bhargava and Sheldarkar, 1993b) is often used for heterogeneous surface energy systems. The Freundlich equation is given as:

$$q_e = K_F C_e^{1/n} \tag{4}$$

A linear form of this expression is:

$$\log q_e = \log K_F + \frac{1}{n} \log C_e \tag{5}$$

where K_F is the Freundlich constant and n the Freundlich exponent. K_F and n can be determined from the linear plot of log q_e versus log C_e. The values of the Freundlich constants together with the correlation coefficient are presented in Table 2 and the theoretical

Table 2. Langmuir, Freundlich Temkin and Dubinin-Radushkevich constans.

Langmuir				Freundlich			Temkin			Dubinin-Radushkevich			
K_L (L/g)	a_L (L/mmol)	Q_0 (mmol/g)	r^2	K_F (L/g)	n	r^2	B	A (L/g)	r^2	q_m (mmol/g)	β (mmol^2/J^2)	E (kJ/mmol)	r^2
18	13.28	1.355	0.999	1.362	3.542	0.859	0.241	226.2	0.930	1.362	2×10^{-8}	5	0.985

Freundlich equation is shown in Fig. 1. The value of correlation coefficient is much lower than the other three isotherm values. In all cases, the Freundlich equation represents the poorest fit of experimental data than the other isotherm equation (Fig. 1).

3.1.3. The Temkin Isotherm. The Temkin isotherm (Choy et al., 1999) has been used in the following form:

$$q_e = \frac{RT}{b}\ln(AC_e) \tag{6}$$

A linear form of the Temkin isotherm can be expressed as:

$$q_e = \frac{RT}{b}\ln A + \frac{RT}{b}\ln C_e \tag{7}$$

where

$$\frac{RT}{b} = B$$

The sorption data can be analyzed according to Eq. (7). Therefore a plot of q_e versus $\ln C_e$ enables one to determine the constants A and b. The values of the Temkin constants A and B are listed in Table 2 and the theoretical plot of this isotherm is shown in Fig. 1. The correlation coefficient is also listed in Table 2 and is higher than the Freundlich value but lower than Langmuir value. Therefore, the Temkin equation only represents a better fit of experimental data than the Freundlich equation but not in the cases of both Langmuir and Dubinin-Radushkevich equations (Fig. 1).

3.1.4. The Dubinin-Radushkevich Isotherm. The Dubinin-Radushkevich isotherm and the Langmuir isotherm equations have been used for the sorption of metal ions on surfactant-modified montmorillonite and sorption of acid dyes on activated carbon (Lin and Juang, 2002; Choy et al., 1999). The Dubinin-Radushkevich equation has the following form

$$q_e = q_m e^{-\beta\varepsilon^2} \tag{8}$$

A linear form of Dubinin-Radushkevich isotherm is:

$$\ln q_e = \ln q_m - \beta\varepsilon^2 \tag{9}$$

where q_m is the Dubinin-Radushkevich monolayer capacity (mmol/g), β a constant related to sorption energy, and ε is the Polanyi potential which is related to the equilibrium concentration as follows

$$\varepsilon = RT\ln\left(1 + \frac{1}{C_e}\right) \tag{10}$$

where R is the gas constant (8.31 J/mol K) and T is the absolute temperature. The constant β gives the mean free energy, E, of sorption per molecule of the sorbate when it is transferred to the surface of the solid from infinity in the solution and can be computed using the relationship (Lin and Juang, 2002; Choy et al., 1999):

$$E = \frac{1}{\sqrt{2\beta}} \tag{11}$$

The Dubinin-Radushkevich constants are calculated and given in Table 2 and the theoretical Dubinin-Radushkevich isotherm is plotted in Fig. 1 together with the experimental data points. Also, the correlation coefficient has been determined and is shown in Table 2 and the value of correlation coefficient is higher than both Freundlich and Temkin values but lower than Langmuir value. Therefore, the Dubinin-Radushkevich equation represents a better fit of experimental data than both Freundlich and Temkin equations but not in the case of Langmuir equation (Fig. 1).

3.2. Kinetic Studies

Figure 2 shows that the amount of phosphorus adsorption increases with time and it remains constant after a contact time of about 120 min (i.e. the equilibrium time). The equilimrium time is independent of initial phosphorus concentration. The time profile of

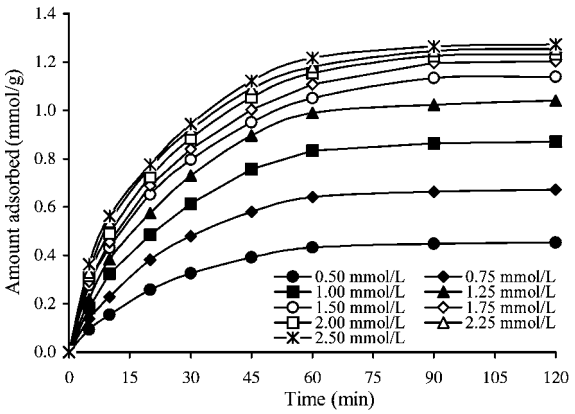

Figure 2. Adsorption kinetics of phosphorus on calcined alunite at different initial concentration. Conditions: 90–150 μm particle size, 1073 K and 30 min calcination, 1 g/100 mL dose, 298 K temperature and pH5.

phosphorus uptake is a single, smooth, and continuous curve leading to saturation, suggesting the possible monolayer coverage of phosphorus on the surface of the adsorbent.

In order to examine the mechanism of adsorption process such as mass transfer and chemical reaction, a suitable kinetic model is needed to analyze the rate data. Many models such as homogeneous surface diffusion model, pore diffusion model, and heterogeneous diffusion model (also known as pore and diffusion model) have been extensively applied in batch reactors to describe the transport of adsorbates inside the adsorbent particles (Wu et al., 2001a; Raven et al., 1998). The large number and array of different functional groups on the calcined alunite surface (e.g., Al_2O_3, SiO_2, etc.) imply that there are different types of adsorbent-adsorbate interactions. Any kinetic or mass transfer representation is likely to be global. From a system design viewpoint, a lumped analysis of kinetic data is hence sufficient for practical operations.

3.2.1. Pseudo First-Order Model. The sorption kinetics may be described by a pseudo first-order equation (Annadurai et al., 2002; Özacar and Şengil, 2002; Wu et al., 2001a–c; Ho and Chiang, 2001). The differential equation is the folowing:

$$\frac{dq_t}{dt} = k_1(q_e - q_t) \tag{12}$$

After integration by applying the initial conditions $q_t = 0$ at $t = 0$ and $q_t = q_t$ at $t = t$, Eq. (12) becomes:

$$\log\left(\frac{q_e}{q_e - q_t}\right) = \frac{k_1}{2.303}t \tag{13}$$

Equation (13) can be rearranged to obtain a linear form:

$$\log(q_e - q_t) = \log q_e - \frac{k_1}{2.303}t \tag{14}$$

where q_e and q_t are the amounts of phosphorus adsorbed at equilibrium and at time t (mmol/g), respectively, and k_1 is the equilibrium rate constant of pseudo first-order adsorption, (1/min).

Figure 3 shows a plot of linearized form of pseudo first-order model at all concentrations studied. The slopes and intercepts of plots of log $(q_e - q_t)$ versus t were used to determine the first-order rate constant k_1 and equilibrium adsorption density q_e. However, the experimental data deviated considerably from the theoretical data. A comparison of the results with the correlation coefficients is shown in Table 3. The correlation

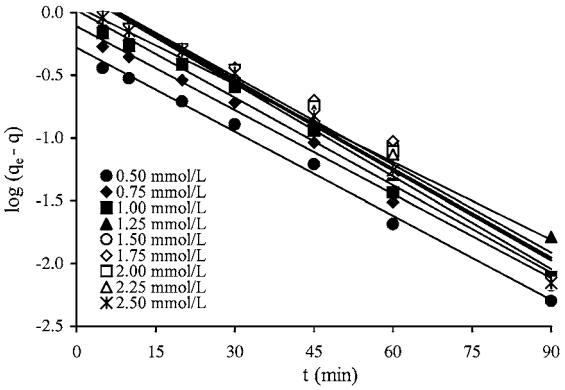

Figure 3. Plot of the pseudo first-order adsorption kinetics of phosphorus on calcined alunite at different initial concentration.

coefficients for the first-order kinetic model obtained at all the studied concentrations were low. Also the theoretical q_e values found from the first-order kinetic model did not give reasonable values. This suggests that this adsorption system is not a first-order reaction.

3.2.2. Pseudo Second-Order Model. The adsorption kinetics may also be described by a pseudo second-order equation (Chiou and Li, 2002; Wu et al., 2001a–c; Ho and Chiang, 2001; Ho and McKay, 1999b). The differential equation is the following:

$$\frac{dq_t}{dt} = k_2(q_e - q_t)^2 \tag{15}$$

Integrating Eq. (15) and applying the boundary conditions, gives:

$$\frac{1}{(q_e - q_t)} = \frac{1}{q_e} + k_2 t \tag{16}$$

Equation (16) can be rearranged to obtain a linear form:

$$\frac{t}{q_t} = \frac{1}{k_2 q_e^2} + \frac{1}{q_e}t \tag{17}$$

where k_2 is the equilibrium rate constant of pseudo second-order adsorption (g/mmolmin).

The slopes and intercepts of plots t/q_t versus t were used to calculate the second-order rate constants k_2 and q_e. The straight lines in plot of t/q_t versus t (Fig. 4) show good agreement of experimental data with the second-order kinetic model for different initial phosphorus concentrations. Table 3 lists the computed results obtained from the second-order kinetic model.

Table 3. Comparison of the first- and second-order adsorption, and intraparticle diffusion rate constants, and calculated and experimental q_e values for different initial phosphorus concentrations.

		First-order kinetic model			Second-order kinetic model			Intraparticle diffusion	
C_o (mmol/L)	$q_{e,\exp}$ (mmol/g)	k_1 (1/min)	$q_{e,\text{cal}}$ (mmol/g)	r^2	k_2 (g/mmol · min)	$q_{e,\text{cal}}$ (mmol/g)	r^2	k_p (mmol/g · min$^{1/2}$)	r^2
0.50	0.453	5.14×10^{-2}	0.525	0.994	8.00×10^{-2}	0.480	0.993	6.33×10^{-2}	0.989
0.75	0.672	5.14×10^{-2}	0.777	0.994	5.40×10^{-2}	0.705	0.993	9.38×10^{-2}	0.989
1.00	0.871	5.37×10^{-2}	1.048	0.991	4.40×10^{-2}	0.915	0.994	11.92×10^{-2}	0.993
1.25	1.041	4.77×10^{-2}	1.122	0.992	3.63×10^{-2}	1.070	0.994	14.15×10^{-2}	0.993
1.50	1.139	5.44×10^{-2}	1.487	0.956	3.63×10^{-2}	1.160	0.998	14.22×10^{-2}	0.991
1.75	1.203	5.39×10^{-2}	1.552	0.958	3.44×10^{-2}	1.230	0.998	14.99×10^{-2}	0.991
2.00	1.232	5.53×10^{-2}	1.541	0.971	3.75×10^{-2}	1.252	0.998	15.42×10^{-2}	0.989
2.25	1.254	5.48×10^{-2}	1.474	0.977	4.15×10^{-2}	1.275	0.998	15.46×10^{-2}	0.984
2.50	1.272	5.66×10^{-2}	1.476	0.986	4.43×10^{-2}	1.297	0.997	15.59×10^{-2}	0.989

The correlation coefficients for the second-order kinetic model obtained were greater than 0.993 for all concentrations. The calculated q_e values also agree very well with the experimental data. These indicate that the adsorption system studied belongs to the second order kinetic model. The similar phenomena are also observed in adsorption of dye RR189 on cross-linked chitosan beads (Chiou and Li, 2002), in adsorption of dye BB69 and DR227 on activated clay (Wu et al., 2001b) and in adsorption of AB9 on mixed sorbents (activated clay and activated carbon) (Ho and Chiang, 2001).

3.2.3. Intraparticle Diffusion Model. Because Eqs. (12) and (15) can not identify the diffusion mechanisms, the intraparticle diffusion model was also tested (Annadurai et al., 1997, 2002; Wu et al., 2001a; Kumar et al., 1987). The initial rate of the intraparticle diffusion is the following:

$$q_t = f(t^{1/2}) \tag{18}$$

The rate parameters for intraparticle diffusion (k_p) at different initial concentrations are determined using the following equation.

$$q_t = k_p t^{1/2} \tag{19}$$

where k_p is the intraparticle diffusion rate constant, (mmol/gmin$^{1/2}$). Such plots may present a multilinearity (Annadurai et al., 2002; Wu et al., 2001a), indicating that two or more steps take place. The first, sharper portion is the external surface adsorption or instantaneous adsorption stage. The second portion is the gradual adsorption stage, where intraparticle diffusion is rate-controlled. The third portion is the final equilibrium stage where intraparticle diffusion starts to slow down due to extremely low adsorbate concentrations in the solution.

Figure 5 shows a plot of the linearized form of the intraparticle diffusion model at all concentrations studied. As shown in Fig. 5, the external surface adsorption (stage 1) is absent. Stage 1 is completed before 5 min, and then the stage of intraparticle diffusion control (stage 2) is attained and continues from 5 min to 60 min. Finally, final equilibrium adsorption (stage 3) starts after 60 min. The phosphorus is slowly transported *via* intraparticle diffusion into the particles and is finally retained in the micropores. In general, the slope of the line in stage 2 is called as intraparticle

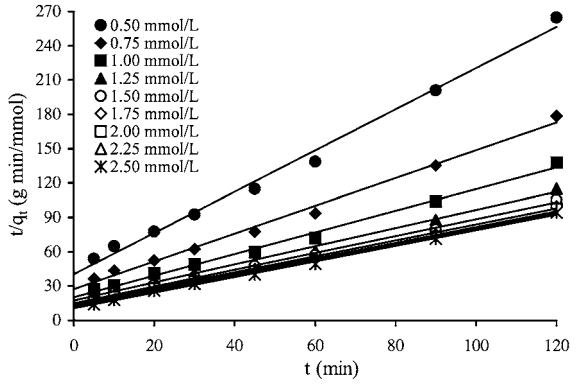

Figure 4. Plot of the pseudo second-order adsorption kinetics of phosphorus on calcined alunite at different initial concentration.

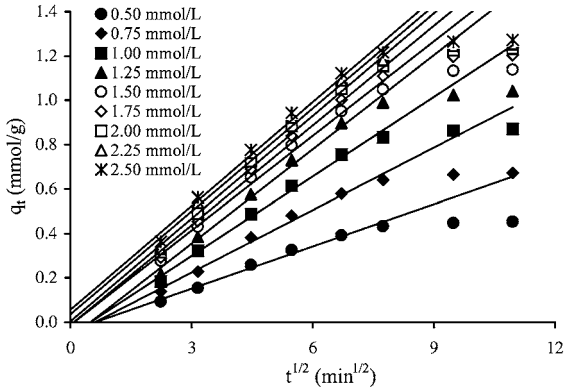

Figure 5. Plot of the intraparticle diffusion model for adsorption of phosphorus on calcined alunite at different initial concentration.

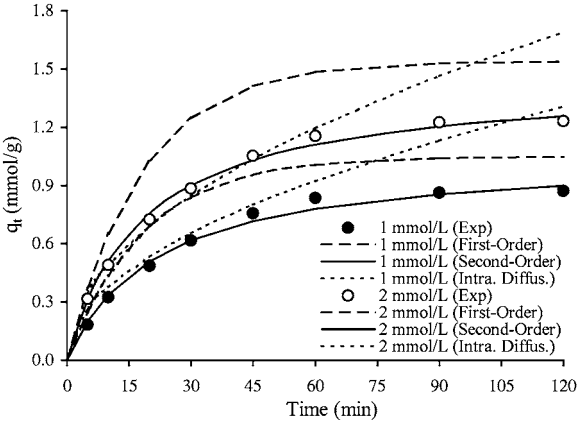

Figure 6. Comparison between the measured and modeled time profiles for adsorption of phosphorus.

diffusion rate constant, k_p. The rate parameters, k_p, together with the correlation coefficients are also listed in Table 3.

A comparison of calculated and measured results for 1.0 and 2.0 mmol/L P concentrations is shown in Fig. 6. As can be seen from Fig. 6, the pseudo second-order kinetic model provides the best correlation for all of the adsorption process, whereas the intraparticle diffusion model fits the experimental data well for an initial period of the adsorption process only. Hence it was concluded that the intraparticle diffusion was found to be rate limiting, followed by the pseudo second-order kinetic model. Similar phenomena are also observed in adsorption of phenols on fly ash (Singh and Rawat, 1994), in adsorption of lead (II) on cypress leaves (Salim et al., 1994), and in adsorption of chrome dye (OCRME) on mixed adsorbents-fly ash and coal (Gupta et al., 1990).

4. Conclusion

Equilibrium and kinetic studies were made for the adsorption of phosphorus from aqueous solutions onto calcined alunite in the concentration range 0.5–2.5 mmol/L at pH 5 and 298 K. The equilibrium data have been analyzed using Langmuir, Freundlich, Temkin and Dubinin–Radushkevich isotherms. The characteristic parameters for each isotherm and related correlation coefficients have been determined. The Langmuir isotherm was demonstrated to provide the best correlation for the sorption of phosphorus onto calcined alunite.

The suitability of the first- and second-order equations, and intraparticle diffusion kinetic model for the sorption of phosphorus onto calcined alunite is also discussed. The adsorption of phosphorus can be described by the intraparticle diffusion model up to 60 min. The intraparticle diffusion model indicates that the external surface adsorption (stage 1) is absent because of completing before 5 min, and final equilibrium adsorption (stage 3) is started after 60 min. The phosphorus is slowly transported *via* intraparticle diffusion into the particles and is finally retained in micropores. The pseudo second-order kinetic model agrees very well with the dynamical behavior for the adsorption of phosphorus onto calcined alunite for different initial phosphorus concentrations over the whole range studied. The reaction mechanism may be partly a result of the complexation or ion exchange between the phosphate molecules and the SiO_2 or Al_2O_3 groups on the calcined alunite surfaces in acidic media.

It may be concluded that alunite may be used as a low-cost, natural and abundant source for the removal of phosphorus and it may be an alternative to more costly materials. It may also be effective in removing as well other harmful or undesirable species such as dyes, present in the waste effluents.

References

Agyei, N.M., C.A. Strydom, and J.H. Potgieter, "An Investigation of Phosphate Ion Adsorption from Aqueous Solution by Fly Ash and Slag," *Cem. Concr. Res.*, **30**, 823–826 (2000).

Annadurai, G., R.-S. Juang, and D.-J. Lee, "Use of Cellulose—Based Wastes for Adsorption of Dyes from Aqueous Solutions," *J. Hazard. Mater.*, **92**, 263–274 (2002).

Annadurai, G. and M.R.V. Krishnan, "Adsorption of Acid Dye from Aqueous Solution by Chitin: Equilibrium Studies," *Indian J. Chem. Tech.*, **4**, 217–222 (1997).

APHA, *Standard Methods for the Examination of Water and Wastewater*, American Public Health Association, American

Water Works association and Water Pollution Control Federation, Washington, DC, 1985.

Bajpai, A.K., M. Rajpoot, and D.D. Mishra, "Static and Kinetic Studies on the Adsorption Behavior of Sulfadiazene," *Adsorption*, **6**, 349–357 (2000).

Baup, S., C. Jaffre, D. Wolbert, and A. Laplanche, "Adsorption of Pesticides onto Granular Activated Carbon: Determination of Surface Diffusivities Using Simple Batch Experiments," *Adsorption*, **6**, 219–228 (2000).

Bhargava, D.S. and S.B. Sheldarkar, "Use of TNSAC in Phosphate Adsorption Studies and Relationships. Literature, Experimental Methodology, Justification and Effects of Process Variables," *Wat. Res.*, **27**(2), 303–312 (1993a).

Bhargava, D.S. and S.B. Sheldarkar, "Use of TNSAC in Phosphate Adsorption Studies and Relationships. Isotherm Relationships and Utility in the Field," *Wat. Res*., **27**(2), 325–335 (1993b).

Brattebø, H. and H. Ødegaard, "Phosphorus Removal by Granular Activated Alumina," *Wat. Res*., **20**(8), 977–986 (1986).

Chiou, M.-S. and H.-Y. Li, "Equilibrium and Kinetic Modelling of Adsorption of Reactive Dyes on Cross-Linked Chitosan Beads," *J. Hazard. Mater.*, **93**(2), 233–248 (2002).

Choy, K.K.H., G. McKay, and J.F. Porter, "Sorption of Acid Dyes from Effluents Using Activated Carbon," *Resources, Conservation and Recycling*, **27**, 57–71 (1999).

Connor, P.A. and A.J. McQuillan, "Phosphate Adsorption onto TiO_2 from Aqueous Solutions: An in Situ Internal Reflection Infrared Spectroscopic Study," *Langmuir*, **15**, 2916–2921 (1999).

Gao, Y. and A. Mucci, "Acid Base Reactions, Phosphate and Arsenate Complexation, and Their Competitive Adsorption at the Surface of Goethite in 0.7 M NaCl Solution," *Geochim. Cosmochim. Acta*, **65**(14), 2361–2378 (2001).

Gong, W., "A Real Time in Situ ATR-FTIR Spectroscopic Study of Linear Phosphate Adsorption on Titania Surfaces," *Int. J. Miner. Process.*, **63**, 147–164 (2001).

Grubb, D.G., M.S. Guimaraes, and R. Valencia, "Phosphate Immobilization Using an Acidic Type F Fly Ash," *J. Hazard. Mater.*, **76**, 217–236 (2000).

Gupta, G.S., G. Prasad, and V.N. Singh, "Removal of Chrome Dye from Aqueous Solutions by Mixed Adsorbents: Fly Ash and Coal," *Wat. Res.*, **24**, 45–50 (1990).

Ho, Y.S. and C.C. Chiang, "Sorption Studies of Acid Dye by Mixed Sorbents," *Adsorption*, **7**, 139–147 (2001).

Ho, Y.S. and G. McKay, "Competitive Sorption of Copper and Nickel Ions from Aqueous Solution Using Peat," *Adsorption*, **5**, 409–417 (1999a).

Ho, Y.S. and G. McKay, "Pseudo-Second Order Model for Sorption Processes," *Process Biochem.*, **34**, 451–465 (1999b).

Huynh, L. and P. Jenkins, "A Rheological and Electrokinetic Investigation of the Interactions Between Pigment Particles Dispersed in Aqueous Solutions of Short-Chain Phosphates," *Colloids and Surfaces A: Physicochem. and Eng. Aspects*, **190**, 35–45 (2001).

Johansson, L. and J.P. Gustafsson, "Phosphate Removal Using Blast Furnace Slag and Opoka-Mechanisms," *Wat. Res.*, **34**(1), 259–265 (2000).

Kumar, S., S.N. Upadhyay, and Y.D. Upadhya, "Removal of Phenols by Adsorption on Fly Ash," *J. Chem. Tech. Biotechnol.*, **37**, 281–290 (1987).

Lin, S.-H. and R.-S. Juang, "Heavy Metal Removal from Water by Sorption Using Surfactant-Modified Montmorillonite," *J. Hazard. Mater.*, **92**, 315–326 (2002).

Onar, A.N., N. Balkaya, and T. Akyüz, "Phosphate Removal by Adsorption," *Environ. Technol.*, **17**(2), 207–213 (1996).

Özacar, M. and İ.A. Şengil, "Adsorption of Acid Dyes from Aqueous Solutions by Calcined Alunite and Granular Activated Carbon," *Adsorption*, **8**, 301–308 (2002).

Raven, K.P., A. Jain, and R.H. Loeppert, "Arsenite and Arsenate Adsorption on Ferrihydrite: Kinetics, Equilibrium, and Adsorption Envelopes," *Environ. Sci. Technol.*, **32**, 344–349 (1998).

Sakadevan, K. and H.J. Bavor, "Phosphate Adsorption Characteristics of Soils, Slags and Zeolite to be Used as Substrates in Constructed Wetland Systems," *Wat. Res.*, **32**(2), 393–399 (1998).

Salim, R., M.M. Al-Subu, and S. Qashoa, "Removal of Lead from Polluted Water Using Decaying Leaves," *J. Environ. Sci. Health Part A Environ. Sci. Eng.*, **29**, 2087–2114 (1994).

Singh, B. and N.S. Rawat, "Comparative Sorption Kinetic Studies of Phenolic Compounds on Fly Ash and Impregnated Fly Ash," *J. Chem. Tech. Biotechnol.*, **61**, 57–65 (1994).

Şengil, İ.A., "The Utilization of Alunite Ore as a Coagulant Aid," *Wat. Res*., **29**(8), 1988–1992 (1995).

Uğurlu, A. and B. Salman, "Phosphorus Removal by Fly Ash," *Environ. Intl.*, **24**(8), 911–918 (1998).

Wu, F.-C., R.-L. Tseng, and R.-S. Juang, "Adsorption of Dyes and Phenols from Water on the Activated Carbons Prepared from Corncob Wastes," *Environ. Technol.*, **22**, 205–213 (2001a).

Wu, F.-C., R.-L. Tseng, and R.-S. Juang, "Kinetics of Color Removal by Adsorption from Water Using Activated Clay," *Environ. Technol.*, **22**, 721–729 (2001b).

Wu, F.-C., R.-L. Tseng, and R.-S. Juang, "Kinetic Modelling of Liquid-Phase Adsorption of Reactive Dyes and Metal Ions on Chitosan," *Wat. Res.*, **35**(3), 613–618 (2001c).